DEVELOPMENT OF A MODAL SUB-STRUCTURING METHOD: APPLICATION TO THERMAL SIMULATIONS OF LNG CARRIERS.

Gaume B.*, Joly F. and Quéméner O.
*Author for correspondence
Laboratoire de Mécanique et d'Energétique d'Evry,
Université d'Evry,
Evry, 91000,
France,
E-mail: b.gaume@iut.univ-evry.fr

ABSTRACT

In the context of simulations of coupled thermal enclosures, we present here a sub-structuring technique adapted to a reduced modal formulation. This technique consists in splitting the geometry into different zones. A modal model is then applied to each zone, and the coupling of the resulting models is performed via a thermal contact resistance. This technique allows the consideration of physical thermal resistances between different components of the geometry, but also the making of fictitious cuts within a continuous domain, when its large size makes it difficult to obtain the global reduced model. Applied to the simulation of a component of a LNG carrier, the use of a sub-structured model with 200 modes allows almost immediate resolution (around 1 second) for a maximum difference near 1 K and an average difference of the order of 0.2 K with respect to a conventional Lagrange finite elements model of shell type, which requires 40 times longer calculation.

INTRODUCTION

Natural gas transportation by LNG tankers represents around 30 % of the total amount of trade movements, which is 330 billion m^3. In order to decrease its volume, the gas is liquefied by lowering its temperature to -163°C. Throughout the crossing of oceans, this low temperature is maintained by containing the liquefied gas in insulated tanks. A LNG carrier is made of several tanks separated by mechanical retaining elements named cofferdams (See Fig. 1). Cofferdams are composed of several metallic enclosures and numerous stiffeners to reinforce the structure.

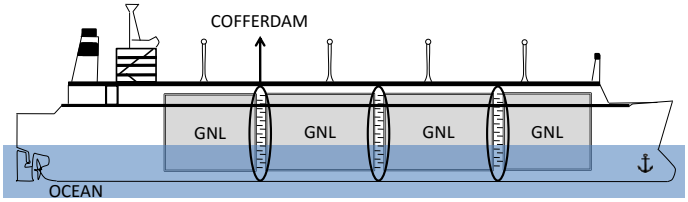

Figure 1 : Schematic view of a LNG tanker

Located between two tanks of LNG at -163°C, each cofferdam is equipped with a heating device to avoid that the temperature of the plates becomes too low. Indeed, below a critical temperature, steel becomes brittle, and the ship is in danger.

A major problematic is the failure of the heating device. In order to take the necessary decisions, it is necessary to have a quick access to the prediction of the entire temperature field to locate the cold spots.

Facing the gigantic size of LNG carriers, conventional computation methods as Lagrange finite elements are too costly in terms of computation time. To comply with the above specifications, the size of the model has to be reduced while maintaining an acceptable precision on the entire computation domain.

Modal methods [1-2] have already shown their ability to face such problematics, but their counterpart is the costly obtainment of the modal base. To get around this difficulty, we propose here a sub-structuring modal method in which the structure is artificially split into several sub-structures coupled together by contact resistances, real or fictitious.

NOMENCLATURE

c	[$J.m^{-3}.K^{-1}$]	Thermal heat capacity
e	[m]	Wall thickness
h	[$W.m^{-2}.K^{-1}$]	Heat exchange coefficient
k	[$W.m^{-1}.K^{-1}$]	Thermal conductivity
M	[m]	Space coordinates
R_{TC}	[$m^2.K.W^{-1}$]	Interfacial thermal resistance
T	[K]	Temperature
$V_i(M)$	[K]	Mode
$x_i(t)$	[-]	Modal amplitude
z_i	[s^{-1}]	Eigenvalue

Special characters

ε	[K]	Difference between detailed and reduced models
$\bar{\varepsilon}$	[K]	Average difference between models
Ω	[-]	Domain
Γ	[-]	Boundary
ζ	[$J.m^{-2}.K^{-1}$]	Steklov number

Subscripts

d	domain
ext	External boundary conditions
int	Internal boundary conditions
fc	Common border
max	Maximum

Superscripts

(k)	Refers to sub-structure k

PHYSICAL MODEL

The cooling of the cofferdam caused by the failure of the heating system is simulated over a period of 30,000 s. The initial condition is the nominal operating temperature.

External boundary conditions

A schematic view of a simplified cofferdam is given in Fig. 2. It consists of N_e=20 enclosures, each containing 4 stiffeners. The heating system is composed of two steel pipes in which water circulates. The cofferdam walls and stiffeners are characterized by different thicknesses e (1 to 3 cm) and constant thermal characteristics (k = 45 W.m^{-1}.K^{-1}, c = 3.4 MJ.m^{-3}.K^{-1}). The boundary conditions are those from the U.S. Coast Guard (U.S.A. federal agency imposing computing standards) : on the outer surfaces Γ_{ext}, the cofferdam is in contact with the atmosphere (h_{atm} = 14 W.m^{-2}.K^{-1}, T_{atm} = 255 K), sea (h_{sea} = 120 W.m^{-2}.K^{-1}, T_{sea} = 273 K) and the insulated tank containing the LNG (h_{LNG} = 0.2 W.m^{-2}.K^{-1}, T_{LNG} = 110 K). These external thermal loads (atmosphere, sea, tubes and LNG) are globally noted h_{ext} and T_{ext}. Both pipes are initially at the heating temperature (brine at 65 °C). During the shutdown, these tubes are cooled by convective exchange with the surrounding enclosures through which they pass.

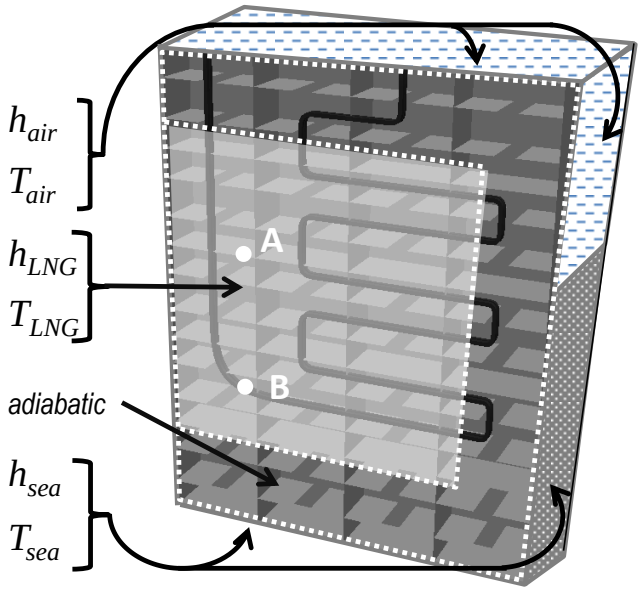

Figure 2 : The cofferdam and its boundary conditions

Internal boundary conditions

As presented in Fig. 3, a convective heat exchange between the inner walls of each enclosure (including the walls of the tubes passing through it) and indoor air (whose temperature $T_{int}^{(e)}$ is unknown and depends on its surroundings) is made via a constant exchange coefficient (h_{int} = 4 W.m^{-2}.K^{-1}). By neglecting the inertia of the air, a simple heat balance on each enclosure yields:

$$T_{int}^{(e)}(T) = \frac{\int_{\Omega_{int}^{(e)}} T \, d\Omega}{\int_{\Omega_{int}^{(e)}} d\Omega} \qquad (1)$$

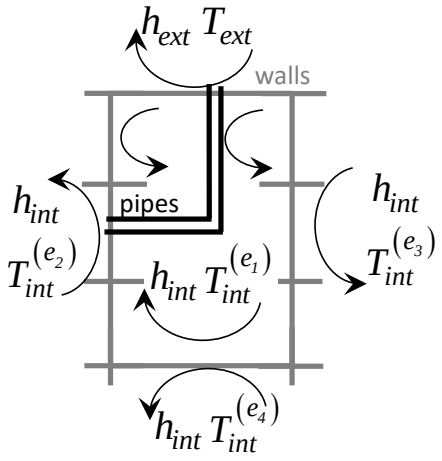

Figure 3 : Boundary conditions of an enclosure

MATHEMATICAL MODEL

Shell hypothesis

Given the thinness of the walls with respect to the other dimensions of the plates forming the cofferdam (several meters), the thermal gradient existing in the thickness is negligible: indeed the Biot number computed in the worst case (h = 120 W.m^{-2}.K^{-1}) is far less than 1. By setting (η, ζ) the local coordinates in the plane defined by the surface Ω_c, a shell model is obtained [3], defined by $T(x, y, z) = T(\eta, \zeta)$.

The sub-structuring method

Let Ω be a closed domain delimited by a boundary Γ. Cutting this domain in N_d sub-structures $\Omega^{(k)}$ reveals a number N_{fc} of common borders with two sub-structures $\Omega^{(i)}$ and $\Omega^{(j)}$ noted $\Gamma_{st}^{(l)}$. On these borders, a temperature jump condition related to a R_{TC} contact resistance is applied, noted $\lceil T \rceil_{(i,j)} = T^{(i)} - T^{(j)}$ (see Fig. 4).

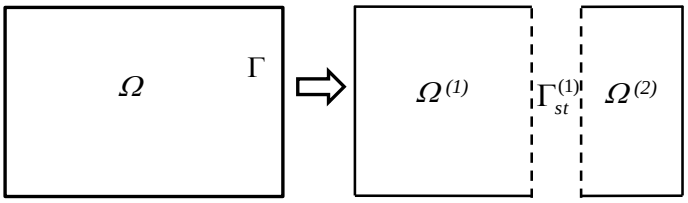

Figure 4 : Initial domain and its sub-structuration

The variational formulation of the heat equation on the entire domain Ω is written as follows:

$$\sum_{k=1}^{N_d}\int_{\Omega_c^{(k)}} e\,c\,\frac{\partial T^{(k)}}{\partial t}\,f^{(k)}\,d\Omega = -\sum_{k=1}^{N_d}\int_{\Omega_c^{(k)}} e\,k\,\vec{\nabla}T^{(k)}\cdot\vec{\nabla}f^{(k)}\,d\Omega$$
$$+\sum_{l=1}^{N_{fc}}\int_{\Gamma_{st}^{(l)}}\frac{e}{R_{TC}}\left\lceil T\right\rceil_{(i,j)}\left\lceil f\right\rceil_{(i,j)}\,d\Gamma$$
$$-\sum_{k=1}^{N_d}\left(\sum_{e=1}^{N_e}\int_{\Omega_{int}^{(k,e)}} h_{int}\,T^{(k)}\,f^{(k)}\,d\Omega\right)$$
$$-\sum_{k=1}^{N_d}\left(\int_{\Omega_{ext}^{(k)}} h_{ext}\,T^{(k)}\,f^{(k)}\,d\Omega\right) \qquad (2)$$
$$+\sum_{k=1}^{N_d}\left(\sum_{e=1}^{N_e}\int_{\Omega_{int}^{(k,e)}} h_{int}\,T_{int}^{(k)}(T)\,f^{(k)}\,d\Omega\right)$$
$$+\sum_{k=1}^{N_d}\left(\int_{\Omega_{ext}^{(k)}} h_{ext}\,T_{ext}\,f^{(k)}\,d\Omega\right)$$

$f^{(k)} \in H_1\left(\Omega^{(k)}\right)$ being test function of sub-structure $\Omega^{(k)}$

The discretization of the problem (2) by Lagrange finite elements brings out the following matrix problem (referred hereafter as detailed model):

$$\begin{aligned}\mathbf{C}\dot{\mathbf{T}} &= \left[\mathbf{K}+\mathbf{J_{st}}+\mathbf{H_{int}}+\mathbf{H_{ext}}\right]\mathbf{T} \\ &+ \mathbf{H_{int}}\mathbf{T_{int}}(\mathbf{T}) + \mathbf{U_0} \\ &= \left[\mathbf{A}+\mathbf{J_{st}}\right]\mathbf{T} + \mathbf{H_{int}}\mathbf{T_{int}}(\mathbf{T}) + \mathbf{U_0}\end{aligned} \qquad (3)$$

Matrix **A** gathers the terms of diffusion and convection for each sub-structure, while matrix $\mathbf{J_{st}}$ comes from the coupling between sub-structures via the contact resistance. $\mathbf{H_{int}}$ matrix corresponds to the convective term with the air inside each enclosure area. $\mathbf{U_0}$ is a vector representing the external known solicitations. The dimension N of Eq. (3) takes into account the temperature jump at the common borders. Denoting $N^{(k)}$ the number of nodes for each sub-structure,

$$N = \sum_{k=1}^{N_d} N^{(k)} \qquad (4)$$

Internal convection

In Eq. (3) $\mathbf{T_{int}}$ is the vector containing the temperature of the air inside each enclosure. As stated above, these temperatures are unknown and depend on the temperature of the cofferdam. The discretization of Eq. (1) yields

$$\mathbf{T_{int}} = \mathbf{U_{cpl}}\,\mathbf{T} \qquad (5)$$

where $\mathbf{U_{CPL}}$ is a matrix of dimension (N_e, N). In order to avoid the manipulation of the full matrix $\mathbf{H_{CPL}} = \mathbf{H_{int}}\mathbf{U_{CPL}}$, incompatible with the finite elements method, Eqs. (3) and (5) are solved iteratively.

In the processed application, a sensitivity analysis showed that a mesh of 21,548 nodes in the cofferdam and 6600 nodes per pipe is required. The resolution of the transient problem over a period of 30,000 s, with variable time steps limited to 100 s, is performed by a CPU time of 60 s. Figure 5 allows to visualize the cooling of the cofferdam and heating pipes for points A and B shown in Figure 1. The inertia due to the heating tubes keeps the temperature of the stiffeners to near 290 K for about an hour, and therefore delays the risk of rupture.

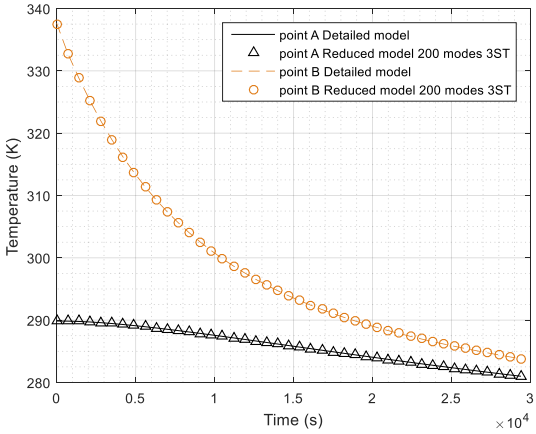

Figure 5 : Temporal evolution of the temperature on points A and B

MODAL METHOD

Principle

In modal methods, the temperature field is searched as a weighted sum of elementary functions named modes:

$$T(M,t) = \sum_{i=0}^{N} V_i(M)\,x_i(t) \qquad (6)$$

Instead of searching for the modes on the whole domain, the idea is to divide the domain in N_d sub-structures, and to compute the modes for each sub-structure [4]. The temperature field will then be searching as

$$T(M,t) = \sum_{k=0}^{N_d}\sum_{i=0}^{N} V_i^{(k)}(M)\;\;x_i^{(k)}(t) \qquad (7)$$

where $V_i^{(k)}$ is a mode defined on sub-structure (k). This can be seen as computing N_d temperature "sub-fields". Obviously, the main difficulty is to link these "sub-fields".

Base branch

The first hurdle is the choice of the modes. A branch base for each body is chosen. This base is the solution of the following eigenvalue problem

$$\forall M \in \Omega^{(k)},\quad k\,\nabla^2 V_i^{(k)} = z_i^{(k)}\,c\,V_i^{(k)} \qquad (8)$$

$$\forall M \in \Gamma^{(k)},\quad k\,\vec{\nabla}V_i^{(k)}\cdot\vec{n} = -z_i^{(k)}\;\zeta\;V_i^{(k)} \qquad (9)$$

where $z_i^{(k)}$ and $V_i^{(k)}$ are respectively the eigenvalues and eigenvectors of the branch base.

This base requires some comments. The first is the special and non-physical boundary condition (9). It is a third type boundary condition in which the heat exchange coefficient *h* (positive) is replaced by an eigenvalue (which is negative), whose value is different for each mode. The second concerns the parameter ζ, the Steklov number, which ensures the dimensional homogeneity of the boundary condition and prevents degeneration of the modal problem.

This special boundary condition reveals two types of modes. The first type is constituted of modes quasi null on the boundary but not on the domain, and the second one of modes quasi null on the domain but not on the boundary. This second type of modes allows to link the temperature "sub-fields" on the interface. Examples of such modes are given in Fig. 6 for the sub-structure $\Omega^{(1)}$ defined in Fig. 4

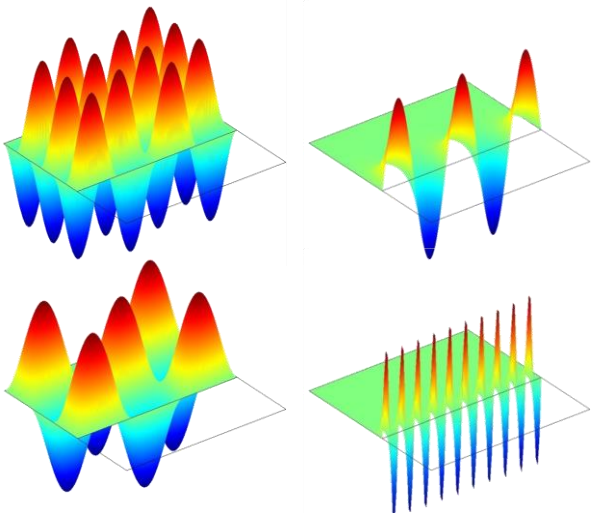

Figure 6 : Examples of branch modes for sub-structure $\Omega^{(1)}$ defined in Fig. 4

Reduction of branch basis using amalgam method

The second hurdle is the reduction in itself. Indeed, the modal formulation only shifts the problem: instead of being temperature values at the nodes of a mesh, the unknowns are the amplitudes of the modes $x_i(t)$. The number of modes needed to approach correctly the solution needs to be reduced. This is done by the amalgam method [5]. In this method, the most influential eigenmodes are kept (they are called major eigenmodes), and the remaining eigenmodes (called minor) are added to them, weighted by a factor. This results in new amalgamated eigenmodes $\tilde{V}_i$, which are a linear combination of eigenvectors of the original branch basis.

$$\tilde{V}_i = \sum_{p=0}^{n_r} \alpha_{i,p} V_{i,p} \qquad (10)$$

The determination of factors $\alpha_{i,p}$ is performed by minimizing the deviation of energy between a reference model and the reduced model.

From the different bases computed on each sub-structure the amalgam method enables to reduce each base corresponding to different sub-structures $\Omega^{(k)}$. This reduction technique produces for each sub-structure a reduced basis $\left(\tilde{z}_i^{(k)}, \tilde{V}_i^{(k)}\right)$. Let $\hat{V}_i^{(k)}$ be the extension of a vector extended by zero to the entire domain Ω. Any temperature field on the entire domain can then be projected on the basis of reduced dimension $\hat{N} = \sum_{1}^{N_d} \tilde{N}^{(k)}$:

$$\begin{aligned} T(M,t) &\approx \sum_{k=1}^{N_d} \sum_{i=1}^{\tilde{N}^{(k)}} \tilde{x}_i^{(k)}(t)\, \tilde{V}_i^{(k)}(M) \\ &\cong \sum_{p=1}^{\hat{N}} \hat{x}_p(t)\, \hat{V}_p(M) \end{aligned} \qquad (11)$$

AMPLITUDE EQUATION AND RESOLUTION OF SUB-STRUCTURED REDUCED PROBLEM

The resolution of the modal problem is carried out in an analogous manner to that used for a single body ([1] [2]). In Eq. (2), the temperature field *T(M,t)* is replaced by its projection in the reduced modal basis (Eq. (11)), and each test function $f^{(k)}$ is expressed as one of the basis vectors $\hat{V}_q$.

As the amplitude equation reveals full matrices of reduced size, the expression of the temperature of the air inside each enclosure $T_{int}^{(e)}$ based on the walls temperature (Eq. (1)) is directly integrated into the heat equation (Eq. (2)), yielding:

$$\begin{aligned} &\sum_{p=1}^{\hat{N}} \sum_{k=1}^{N_d} \int_{\Omega_c^{(k)}} e c \hat{V}_p \hat{V}_q \, d\Omega \frac{d\hat{x}_p}{dt} = \\ &-\sum_{p=1}^{\hat{N}} \sum_{k=1}^{N_d} \int_{\Omega_c^{(k)}} e k \vec{\nabla}\hat{V}_p \vec{\nabla}\hat{V}_q \, d\Omega \, \hat{x}_p \\ &+\sum_{p=1}^{\hat{N}} \sum_{l=1}^{N_{fc}} \int_{\Gamma_{st}^{(l)}} \frac{e}{R_{TC}} \left[\hat{V}_p\right]_{(i,j)} \left[\hat{V}_q\right]_{(i,j)} d\Gamma \, \hat{x}_p \\ &-\sum_{p=1}^{\hat{N}} \sum_{k=1}^{N_d} \left(\sum_{e=1}^{N_e} \int_{\Omega_{int}^{(k,e)}} h_{int} \hat{V}_p \hat{V}_q \, d\Omega \right) \hat{x}_p \\ &-\sum_{p=1}^{\hat{N}} \sum_{k=1}^{N_d} \left(\int_{\Omega_{ext}^{(k)}} h_{ext} \hat{V}_p \hat{V}_q \, d\Omega \right) \hat{x}_p \\ &+\sum_{p=1}^{\hat{N}} \sum_{k=1}^{N_d} \left(\sum_{e=1}^{N_e} \frac{1}{\int_{\Omega_{int}^{(k,e)}} h_{int} \, d\Omega} \int_{\Omega_{int}^{(k,e)}} h_{int} \hat{V}_q \, d\Omega \int_{\Omega_{int}^{(k,e)}} h_{int} \hat{V}_p \, d\Omega \right) \hat{x}_p \\ &+\sum_{k=1}^{N_d} \left(\int_{\Omega_{ext}^{(k)}} h_{ext} T_{ext} \hat{V}_q \, d\Omega \right) \end{aligned} \qquad (12)$$

After discretization, the relationship (12) can be expressed more compactly in matrix form, noting the matrix $\hat{\mathbf{V}}\left[N_{STR},\hat{N}\right]$ defining the reduced base:

$$\left[\hat{\mathbf{V}}^{\mathbf{t}}\mathbf{C}\hat{\mathbf{V}}\right]\frac{d\mathbf{X}}{dt}=\left[\hat{\mathbf{V}}^{\mathbf{t}}\left(\mathbf{K}+\mathbf{J}_{\mathbf{st}}+\mathbf{H}_{\mathbf{int}}+\mathbf{H}_{\mathbf{ext}}+\mathbf{H}_{\mathbf{cpl}}\right)\hat{\mathbf{V}}\right]\mathbf{X}+\hat{\mathbf{V}}^{\mathbf{t}}\mathbf{U}_{\mathbf{0}} \quad (13)$$

RESULTS

Results are presented in terms of computing time and average and maximum temperature deviations from the detailed model in Tables 1 and 3 for different domain separations, different boundary conditions and different reduction orders. Two configurations are tested. The first corresponds to the reference case used for the reduction process by amalgam (β = 1), while in the second one all the exchange coefficients are increased by a factor β = 1.4.

SUB STRUCTURATION FOR PHYSICAL THERMAL RESISTANCES

Initially, the division into sub-structures follows the physical division, *i.e.* the cofferdam (ST1) and the two heating pipes (ST2 and ST3). The thermal resistance between the different sub-structures has a physical reality and is estimated to R_{TC} = 1W^{-1}.m^2.K. Different modal simulations are carried out keeping 40 modes for each heating tube, and varying the number of modes for the cofferdam. The construction of the modal model (computation of the base and reduction), is performed offline and requires a calculation time of 1582 s.

When the boundary conditions for the simulation match those used for reduction (β = 1) the difference between reduced and detailed models is already very low with only 120 modes (compared to 34,748 nodes of the initial mesh), with a maximum deviation of 0.7 K, an average deviation of 0.03 K, and a gain in term of computation time upper than 60, thus showing the effectiveness of the method for problems characterized by structures coupled by a thermal contact resistance.

model order (ST_1 ST_2 ST_3)	$\beta=1$			$\beta=1{,}4$		
	t_{CPU}(s)	ε_{max} (K)	$\bar{\varepsilon}$ (K)	t_{CPU}(s)	ε_{max} (K)	$\bar{\varepsilon}$ (K)
120 (40 - 2×40)	0.99	0.73	0.031	1.08	1.82	0.149
140 (60 - 2×40)	1.17	0.40	0.021	1.25	1.23	0.135
160 (80 - 2×40)	1.44	0.33	0.016	1.50	0.83	0.114
200 (120 - 2×40)	2.15	0.18	0.010	2.23	0.82	0.089
240 (160 - 2×40)	2.80	0.17	0.007	2.93	0.63	0.071

Table 1: *maximum and average absolute error for different reduction orders for 3 ST*

When the boundary conditions are different from those used during reduction (β = 1.4) performance degrades, and even with 240 modes, the maximum deviation is greater than 0.5 K for a gain in computation time of 20. This deterioration has yet to be put into perspective, since even with a model with 120 degrees of freedom, the maximum deviation is less than 2 K and the average difference is less than the sensitivity of a thermocouple.

SUB STRUCTURATION WITH FICTITIOUS THERMAL RESISTANCE

In addition to the two pipes, the cofferdam has been artificially divided into 4 sub-structures shown in Figure 7 and coupled together by an artificial contact resistance. It is then checked if the method is able to reduce such a problem.

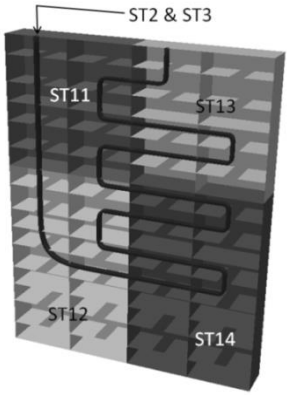

Figure 7 : Virtual division of the cofferdam

The first step is to find an optimal value for the fictitious thermal contact resistance. Indeed, an excessive value of the fictitious resistance biases results by introducing a too important non-physical temperature jump. On the other hand, due to the reduction of the modal base, impose a too low temperature jump at the interface induces a significant error in the calculation of the heat flux, and therefore significant temperature differences either in the interface, but also in the domain. A sensitivity analysis on the value of the R_{TC} has been conducted for different orders of reduction. Results are presented in Table 2.

Nb of modes	240 (4×40- 2×40)		160 (4×20- 2×40)		120 (4×10- 2×40)	
R_{TC}	$\bar{\varepsilon}(K)$	$\varepsilon_{max}(K)$	$\bar{\varepsilon}(K)$	$\varepsilon_{max}(K)$	$\bar{\varepsilon}(K)$	$\varepsilon_{max}(K)$
10^{-3}	0.095	2.72	0.128	2.35	0.162	2.12
2.10^{-4}	0.076	0.96	0.119	1.06	0.158	2.06
10^{-4}	0.076	0.96	0.123	1.01	0.165	1.92
5.10^{-5}	0.078	0.97	0.128	0.97	0.176	1.70
2.10^{-5}	0.083	1.02	0.137	1.57	0.195	1.82
10^{-5}	0.088	1.07	0.144	2.37	0.212	2.09
5.10^{-6}	0.094	1.13	0.153	3.25	0.233	3.19
10^{-6}	0.116	1.73	0.183	5.47	0.353	6.61

Table 2*: Influence of the value of the fictitious contact resistance on the accuracy of the model*

It is first noted that, for a given reduction order, depending on the chosen criterion ($\bar{\varepsilon}(K)$ or $\varepsilon_{max}(K)$) the optimum value of the contact resistance is not the same. In addition, the optimum value for a given criterion changes depending on the order of reduction. However, we also note that there is a whole range (roughly $5.10^{-5}<R_{TC}<10^{-4}$ W^{-1}.m^2.K.) on which the change in

spreads is low, indicating that an order of magnitude is sufficient. The value R_{TC}= 10^{-4} $W^{-1}.m^2.K$ has been chosen.

Reduced model order (ST_{11}, ST_{12}, ST_{13}, ST_{14}, ST_2,ST_3)	$\beta = 1$			$\beta = 1{,}4$		
	t_{CPU}(s)	$\varepsilon_{max}(K)$	$\bar{\varepsilon}(K)$	t_{CPU}(s)	$\varepsilon_{max}(K)$	$\bar{\varepsilon}(K)$
120 (4×10- 2×40)	0.68	1.29	0.060	0.71	1.92	0.165
140 (4×15- 2×40)	0.83	0.93	0.045	0.82	2.30	0.143
160 (4×20- 2×40)	0.97	0.66	0.033	0.89	1.04	0.123
200 (4×30- 2×40)	1.10	0.47	0.019	1.18	1.07	0.093
240 (4×40- 2×40)	1.31	0.32	0.014	1.36	0.96	0.076

Table 3: *maximum and average absolute error for different reduction orders for 6 ST*

Figure 8 shows the time evolution of the difference between reduced and detailed model at points A and B (see Figure 2) for both divisions (physical and artificial) with 200 modes. It clearly appears that the error is larger for the first steps of simulation and tends to stabilize at a value less than 0.1K. When both divisions are compared following the number of modes, the second splitting seems less relevant, since for β = 1 and 160 modes, for example, maximum and average deviations are about 2 times higher. This is easily explained: as each sub-structure requires a minimum number of modes to reproduce a temperature field, increasing the number of sub-structures increases the total number of modes.

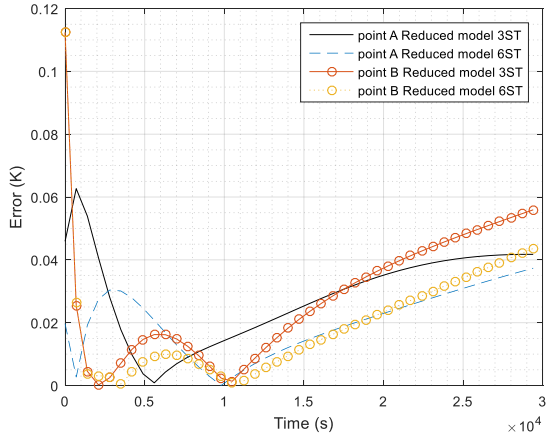

Figure 8 : Temporal evolution of the deviation between detailed and reduced model

However, when this comparison is made based on the computation time, the reduced model of order 160 of the artificial splitting must rather be compared to the reduced model of order 120 of the physical splitting, where the differences are of the same order of magnitude. This is also true in the case β = 1.4, for which a model with 3 subdomains and 140 modes is simulated in a time equal to a model with 6 sub-structures and 200 modes. The results in terms of precision are then substantially equal.

This difference in computation time between models of the same order (and thus problems between matrices of the same size) reflects the structure of matrices and the employed resolution algorithm. The matrix resolution is achieved by BLAS and LAPACK libraries, which use a partition block matrices. The matrix structure of the sub-structured problem lends itself to this kind of partition since the sub-structuring naturally reveals zero blocks corresponding to sub-structures that are not coupled together. The major advantage of this new division comes from the computation time taken to build the modal model, since it is simpler and faster to solve N_d problems of dimension $[N^{(k)} \times N^{(k)}]$ rather than one problem of dimension $[N \times N]$. Thus, by cutting artificially the cofferdam, the computation time required for the construction of the model decreases from 1582 s to 418 s, which is almost a factor 4.

CONCLUSION

The first objective of this communication was the study of a sub-structured reduced model for a geometry made up of many thermal enclosures coupled together when the imperfect contact between different components reveals a temperature jump at the interface. We have shown the efficiency of this method, since for a different problem than the reference one, the maximum deviation from Lagrange finite element model is less than 1 K, while being 40 times faster. However the price is getting the initial basis on which is built the amalgamated basis.

The second objective was to study the relevance of this technique for an artificial division of an initially continuous domain. Results are very satisfactory, since we find the same ratio precision - computation time, while dividing the time to create the reduced model by a factor 4. This study thus demonstrated the effectiveness of the sub-structured modal method, which could be extended to the cofferdam in all its geometrical complexity, and all of the ship's structure.

Acknowledgement: The authors wish to thank **GazTransport & Technigaz** for its financial support**.**

REFERENCES

[1] E. Videcoq, A. Neveu, O. Quemener, M. Girault, D. Petit, Comparison of two non-linear model reduction techniques : The modal identification method and the branch eigenmodes reduction method. Num Heat Transfer B, 49 (2006), 537–558

[2] D. Alonso, A. Velazquez, J.M. Vega, Robust reduced order modeling of heat transfer in a back step flow, Int. J. Heat and Mass Transfer, 52 (2009), 1149–1157

[3] A. E. Jeffers, Heat transfer element for modeling the thermal response of non-uniformly heated plates. Finite Elements in Analysis and Design 63 (2013), 62–68

[4] P. O. Laffay, O. Quemener, A. Neveu, Developing a method for coupling branch modal models, IJTS, 48 (2009), 1060–1067.

[5] O. Quéméner, F. Joly, and A. Neveu, The generalized amalgam method for modal reduction, Int. J. Heat and Mass Transfer, 55 (2012), 1197–1207